JMEPEG (1993) 2:645-650

The Effect of Pressure on the Combustion Synthesis of a Functionally-Graded Material: TiB_2-Al_2O_3-Al Ceramic-Metal Composite System

H.J. Feng and J.J. Moore

This article describes some recent research on the synthesis of functionally-graded materials (FGM) using combustion synthesis or self-propagating high-temperature synthesis (SHS). A model ceramic-metal SHS system was investigated based on the reaction system:

$$3TiO_2 + 3B_2O_3 + (10 + x)Al = 3TiB_2 + 5Al_2O_3 + xAl$$

in which x was varied between 0 and 17 to achieve the required composition and phase gradients in the FGM. The effects of combustion mode, reactant stoichiometry (xAl), green density, and applied loads on the stability of the SHS reaction and density of the FGM product are described.

Keywords
aluminum, functionally-graded materials, self-propagating high-temperature synthesis

1. Introduction

COMBUSTION synthesis, or self-propagating high-temperature synthesis (SHS), is currently being investigated as a potential economic route for producing numerous advanced ceramic composite materials.[1]

Combustion synthesis relies on the ignition of an exothermic reaction mixture in a compacted powder form, e.g., pellet, such that the heat generated from the reaction renders the reaction system to be self-sustaining. Once the exothermic reaction is initiated, the reaction front moves rapidly through the compacted powder mix, producing the required product.

A model functionally-graded material (FGM) ceramic-metal composite has been investigated based on the TiB_2-Al_2O_3-Al system discussed in an earlier paper.[2] In this material an excess amount of Al is used to produce the liquid metal that infiltrates the porous ceramic TiB_2-Al_2O_3 matrix and also provides the compositional gradient in the FGM composite, i.e.:

$$3TiO_2 + 3B_2O_3 + (10 + x)Al = 3TiB_2 + 5Al_2O_3 + xAl \quad [1]$$

2. Experimental Procedure

The reactant powders of TiO_2 (–44 μm), B_2O_3 (–75 μm), and Al (–44 μm) were thoroughly mixed using porcelain ball milling for 4 h and then pressed, using varying amounts of excess Al, into pellets of the configuration shown in Fig. 1.

H.J. Feng and **J.J. Moore**, Department of Metallurgical and Materials Engineering, Colorado School of Mines, Golden, Colorado.

The functionally-graded material was prepared as a compacted green pellet in which the excess amount of Al in Reaction 1 was varied from $x = 0$ at the top to $x = 17$ at the bottom of the pellet. Therefore, the stoichiometry of the top of the pellet was $3TiB_2 + 5Al_2O_3$ and that at the bottom was $3TiB_2 + 5Al_2O_3 + 17Al$. Two intermediate layers in which $x = 5$ and $x = 10$ were also included in this FGM. The four equal volume compositional sections were pressed to the same green density for each FGM. However, different green densities were investigated for four different FGM pellets, i.e., the reactant powders were pressed using four different cold pressing pressures of 2.6×10^6 kg/m^2, 1.6×10^7 kg/m^2, 3.9×10^7 kg/m^2, and 6.3×10^7 kg/m^2.

The combustion synthesis reaction was conducted in a fused quartz reaction chamber so that the propagation of the combustion front along the pellets could be recorded using a video camera. An electrically heated tungsten filament was used to ignite these pellets in the propagating mode in an argon atmos-

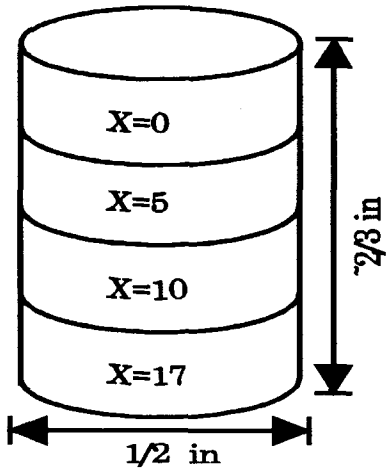

Fig. 1 FGM reactant powder assembly.

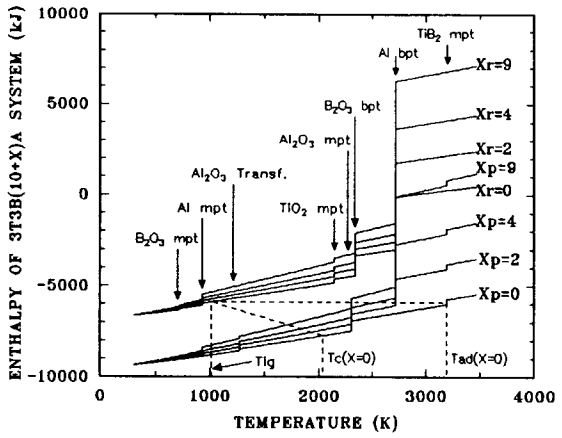

Fig. 2 Enthalpy-temperature plot for reactants (*Xr*) and products (*Xp*) for the reaction $3TiO_2 + 3B_2O_3 + (10 + x)Al = 3TiB_2 + 5Al_2O_3 + xAl$ for various amounts of excess Al, i.e., *Xr*, *Xp* = 0, 5, 10, and 17. The melting (mpt) and boiling (bpt) points of various reactants and products are also indicated on the plots.

phere; the distance between the tungsten coil and the top surface of the green pellet was kept constant to provide similar heating rates for each reaction system. The ignition temperatures, T_{ig}, were determined using a Pt-Pt/10%Rh thermocouple, and the combustion temperatures, T_c, were determined using an IRCON mirage two-wavelength infrared pyrometer that was checked with a W-W/5%Re thermocouple.

The degree of completion of the reaction was checked using X-ray diffraction (XRD), which was also used to determine whether the desired products were produced. The synthesized

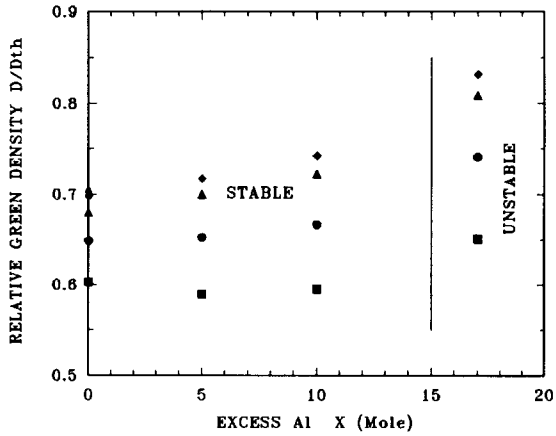

Fig. 3 Propagation wave stability diagram for the SHS reaction $3TiO_2 + 3B_2O_3 + (10 + x)\,Al = 3TiB_2 + 5Al_2O_3 + xAl$.

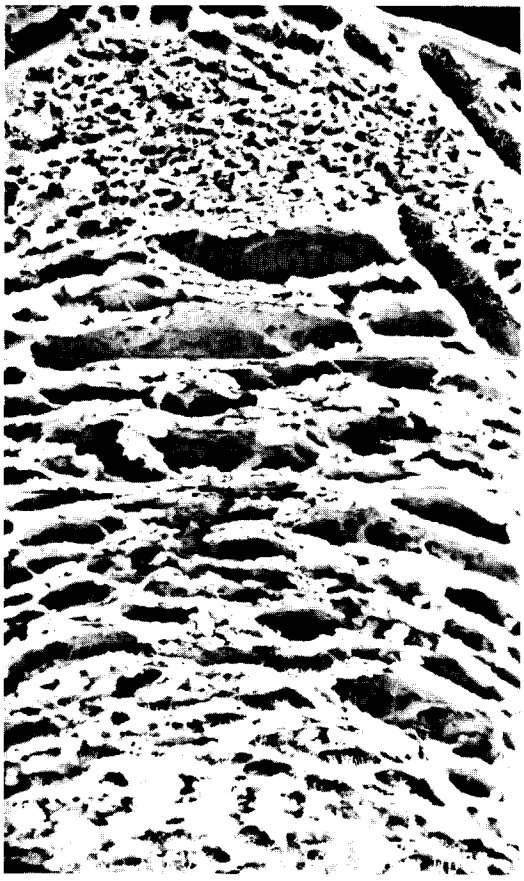

(a)

(b)

Fig. 4 SEM photomicrographs of ceramic-metal composite $3TiO_2 + 3B_2O_3 + (4 + x)Al = 3TiB_2 + 2Al_2O_3 + xAl$ in which the green compaction pressure was 2.6×10^7 kg/m^2 for (a) $x = 5$ and (b) $x = 10$.

FGM materials were examined using optical and scanning electron microscopy (SEM) interfaced with an energy dispersed analysis point X-ray (EDAX) facility. The porosity of the products was characterized with respect to the volume fraction of open, closed, and total pores using a simple water immersion technique. From these data, the theoretical relative density of the FGM products was determined.

Figure 2 provides the enthalpy-temperature relationship for Reaction 1, in which *Xr* and *Xp* refer to the respective reactant and product *H-T* plots associated with the corresponding ex-

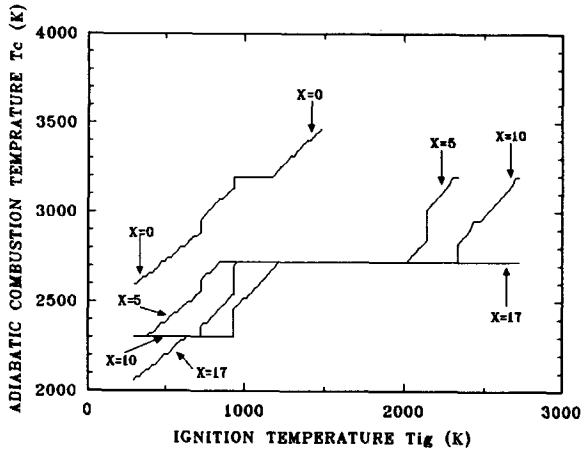

Fig. 5 Effect of ignition temperature, T_{ig}, and excess Al (xAl) on the theoretical adiabatic temperature of Reaction 1.

Table 1 Physical properties of reactants and products used in Reaction 1

Property	TiO_2	Al	Al_2O_3	B_2O_3	TiB_2
Melting point, °C.....	1830	660	2072	450	2900
Boiling point, °C.....	3000	2467	2980	1860	...
Specific gravity.....	4.26	2.70	3.97	2.46	4.50

(a)

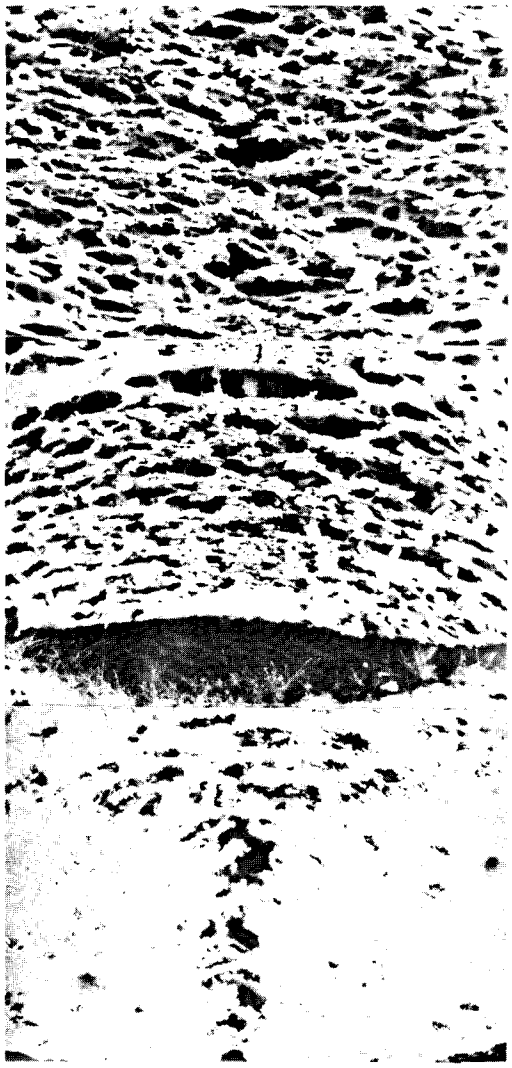

(b)

Fig. 6 Macrostructure of $3TiB_2$-$5Al_2O_3$-xAl FGM produced under the propagating mode with a green compaction pressure of (a) 1.6×10^7 kg/m^2 and (b) 3.95×10^7 kg/m^2.

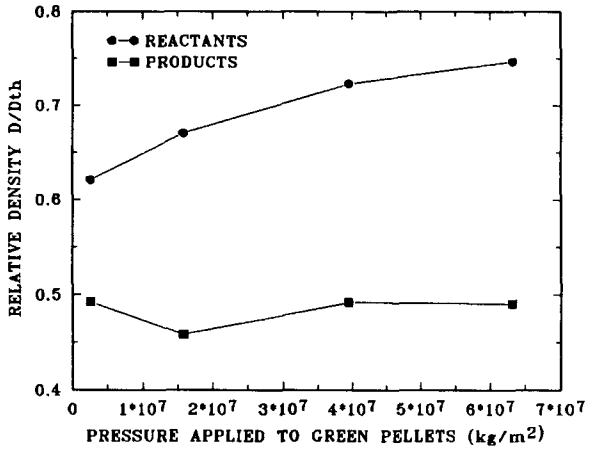

Fig. 7 Effect of green pressure on relative density of reactants and products for the combustion synthesis of the $3TiB_2$-$5Al_2O_3$-xAl FGM reacted under the propagating mode.

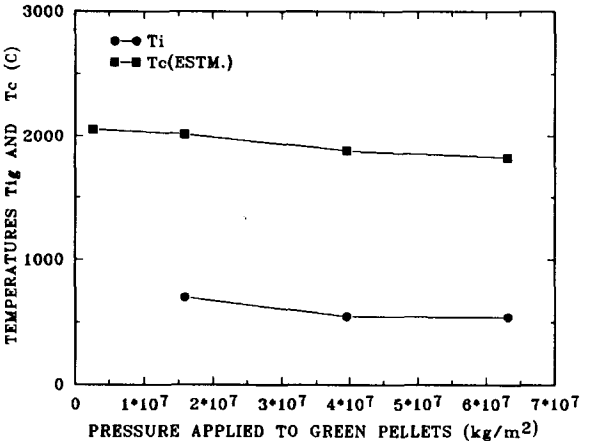

Fig. 8 Effect of green pressure on T_{ig} and T_c (estimated average) from the $3TiB_2$-$5Al_2O_5$-xAl FGM reacted under the propagating mode.

cess amount of Al (xAl), e.g., $Xr = 5$ and $Xp = 5$ refer to the stoichiometry where there are 5 moles of excess Al produced to infiltrate the porous ceramic matrix. Also indicated on this diagram and in Table 1 are the corresponding melting and boiling points of reactants and products. The effect of excess Al and green density on the stability of the reaction front was determined earlier[2] and given in Fig. 3. The maximum theoretical product density of approximately 75% was achieved with an excess Al of 10 moles for Reaction 1 at a load of $\leq 1.6 \times 10^7$ kg/m^2 applied to the green pellet reactant mix. For the reaction mixture in which $x = 0$, although the porosity was extensive, e.g., 63% by volume, it was predominately open pore porosity, i.e., in excess of 60% by volume. Figure 4 provides SEM photomicrographs of the cross section of the ceramic-metal composites produced from previous work[2] when the green pellet (not in FGM form) was pressed under a green load of 2.6×10^6 kg/m^2 for (a) $x = 5$ and (b) $x = 10$. The ability of the liquid Al to fill the pores in the ceramic matrix is evident.

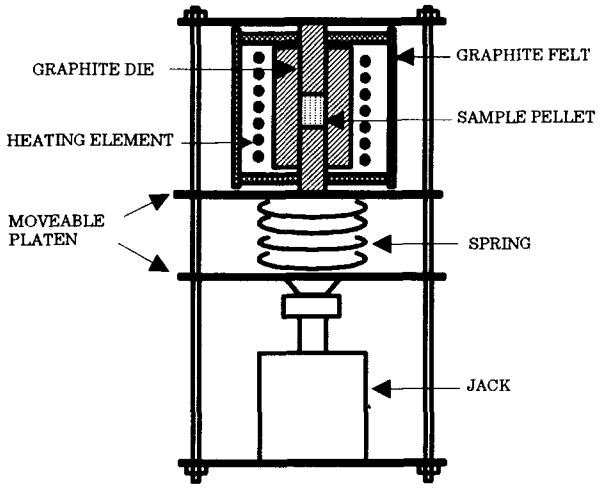

Fig. 9 Schematic of the combustion system reaction chamber with spring-loaded platen.

The theoretical effect of T_{ig} and excess Al on T_{ad} is given in Fig. 5, as calculated using the Kirchoff equation in which T_o is the initial or starting temperature, e.g., 298 K:

$$\Delta H(T_{ad}) = \Delta H(T_o) + \int_{T_o}^{T_{trans}} CpdT \pm \Delta HT_{trans} + \int_{T_{trans}}^{T_{ad}} Cpdt \quad [2]$$

where T_{trans} is the temperature of a phase change occurring in one of the reactants or products, and ΔHT_{trans} is the associated heat of transformation in a reactant (+) or product (–). In Reaction 1, there are several phase changes in both reactants and products, and these phase changes are reflected in Fig. 1 and 5. The presence of gaseous reactants, i.e., B_2O_3 and Al, has been shown to result in the formation of Al_2O_3 whiskers in the pores and open surfaces of the TiB_2-based ceramic matrix.[2]

3. Results and Discussion

Initially, the green FGM reaction mixtures were ignited using a flat tungsten coil in the propagating mode as described above. The macrostructures of some typical FGM products are shown in Fig. 6. Note the whiskers in the large radial pore in Fig. 6(b). The effect of the initial green density on the final product density is given in Fig. 7. Table 2 provides the data for all four FGM samples investigated. It is apparent from Fig. 6 and 7 that the initial green density did not significantly affect the final overall product density. The ceramic-metal FGM product exhibited a highly porous top section, a large radial gas hole just below the center, and a solid dense bottom section that contained the maximum excess Al. However, those FGM samples compacted to green densities in excess of 1.6×10^7 kg/m^2 exhibited increased porosity even in the bottom section, i.e., $x = 17$. This is in agreement with the previous work reported [2] for this reaction system.

(a)

(b)

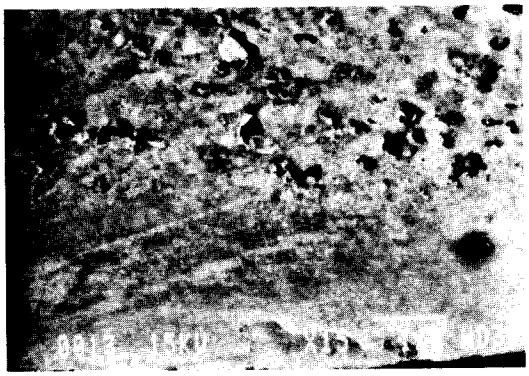

(c)

(d)

Fig. 10 SEM macrostructure of $3TiB_2$-$5Al_2O_3$-xAl FGM reacted under the thermal explosion mode with (a) no squeezing during the combustion synthesis reaction and a green compaction load of 1.6×10^7 kg/m^2, (b) ≤100 psi squeezing pressure and a green compaction load of 2.6×10^6 kg/m^2, (c) ≤150 psi squeezing pressure and green compaction load of 6.3×10^7 kg/m^2, and (d) ≤200 psi squeezing pressure and a green compaction load of 1.6×10^7 kg/m^2.

The effect of green density on T_{ig} and T_c is indicated in Fig. 8. The combustion temperature in this case was taken as the estimated averaged combustion temperature because each section will produce a different theoretical T_{ad}. From these data, it was concluded that some form of compaction is needed to produce dense FGM products using combustion synthesis and that the propagating mode of combustion may not be the ideal mode. The most practical way of providing compaction simultaneously as the combustion synthesis reaction proceeds is to ignite the green FGM composite with a heating coil surrounding the pellet. This necessitates ignition using the simultaneous combustion or bulk mode. Therefore, a tungsten coil was designed so that it surrounded the FGM green pellet, which was enclosed within a spring-loaded platform with graphite felt placed around the tungsten coil, as indicated in Fig. 9. With this design, the maximum compaction load depends on the strength

Table 2 Compaction pressures (P) of green (unreacted) FGMs, relative density of green (Dr/Dth) and reacted (Dp/Dth) FGMs, volume fractions of total (V_T), open (V_O)and closed (V_I) pores in reacted FGM, ignition (T_{ig}), and average combustion (T_c) temperatures. Reacted under propagation mode of combustion.

P, kg/m^2	Dr/Dth	Dp/Dth	V_T	V_O	V_I	T_{ig}	T_c
0.261×10^7	0.62	0.492	0.508	0.326	0.182	...	2051
1.579×10^7	0.67	0.459	0.541	0.399	0.142	700	2016
3.947×10^7	0.72	0.492	0.508	0.416	0.092	545	1880
6.315×10^7	0.75	0.491	0.509	0.388	0.121	540	1827

of the spring. Three different spring strengths were used, and the load on the spring was subsequently measured by compacting the spring on a MTS tensile testing machine to the same position experienced during the combustion synthesis reaction. In this way, it was possible to determine the approximate squeezing compaction loads on each of these four samples. Figure 10 provides the macrostructures of the FGM composites in which a simultaneous compaction load had been applied during the combustion synthesis reaction conducted using the design given in Fig. 9, i.e., 0, ≤100 psi, ≤150 psi, and ≤200 psi.

Comparison of Fig. 10(a) with Fig. 6 provides an interesting comparison of the two modes of ignition, i.e., simultaneous combustion and propagating modes, respectively. The simultaneous combustion mode initiates the exothermic reaction at approximately the same time throughout the entire green FGM compact. This allows the excess liquid metal at the bottom of the compact to rise by capillary action into the middle portions of the pellet, but also provides increased voids and porosity in the top and bottom of the FGM compared with that shown in Fig. 6. It is also apparent that several large radial pores are present in the simultaneous combustion mode sample, whereas only one large radial pore was present when the FGM material was ignited using the propagating mode (Fig. 6). Increasing the strength of the spring that simultaneously squeezed the green FGM composite material during the combustion synthesis reaction increased the product density of the FGM. The significant improvement in density even with compaction loads of <200 psi is a very promising result for the potential production of tough, dense, near-net shaped functionally-graded materials.

4. Conclusions

Combustion synthesis offers an efficient processing route for the synthesis of ceramic-metal functionally-graded materials. Thermal explosion of the green FGM pellet coupled with a light squeezing compaction simultaneously applied while the reaction proceeds offers a means by which the FGM material can be consolidated. Squeezing at pressures as low as 200 psi provided substantial improvements in product density. This combination of combustion synthesis and squeezing is needed to produce dense functionally-graded materials even when the excess liquid metal infiltrant concept is used.

The optimum processing conditions depend on the particular reaction system used. For example, physical properties of the reactants and products, e.g., melting point and boiling point, need to be taken into account because these will substantially affect the combustion temperature and morphology and densification of the product phases. Increasing the green density of the FGM pellet had little effect on the density of the FGM product produced by the propagating mode of combustion and had only a small effect on the ignition and combustion temperatures, i.e., both T_{ig} and T_c decreased slightly with increasing green density.

Acknowledgments

The authors are grateful for the partial support of this work by NASA Microgravity Sciences Division-Code SN.

References

1. Z.A. Munir and U. Anselmi-Tamburine, *Mater. Sci. Rep.*, Vol 3 (No. 7), 1989, p 8

2. H.J. Feng, J.J. Moore, and D.G. Wirth, "Combustion Synthesis of TiB_2-Al_2O_3-Al Ceramic-Metal Composites," *Proceedings of Symposium in Developments in Ceramic and Metal Matrix Composites*, K. Upadhya and J.J. Moore, Ed., TMS, 1992, p 219-239